Desalination and Water Treatment
www.deswater.com

doi: 10.1080/19443994.2013.821042

52 (2014) 6620–6631
October

Taylor & Francis
Taylor & Francis Group

Impact of various physico-chemical parameters on spontaneous nucleation of struvite ($MgNH_4PO_4.6H_2O$) formation in a wastewater treatment plant: kinetic and nucleation mechanism

Eko Ariyanto[a,b], Ha Ming Ang[a], Tushar Kanti Sen[a,]*

[a]*Department of Chemical Engineering, Curtin University, GPO Box U 1987, Perth 6845, Western Australia, Australia*
Tel. +61 8 92669052; Fax: +61 8 92662681; email: t.sen@curtin.edu.au
[b]*Department of Chemical Engineering, Muhammadiyah University of Palembang, Palembang, Indonesia*

Received 19 April 2013; Accepted 10 June 2013

ABSTRACT

In this study, the effect of various physico-chemical parameters such as supersaturation, temperature and pH, and the presence of foreign ion on the nucleation of struvite formation in a wastewater treatment plant were studied experimentally. Mechanism of nucleation kinetics of struvite ($MgNH_4PO_4.6H_2O$) formation has been identified by thermodynamic parameters study. The time taken for nucleation to occur (often indicated by the induction time) is a measure of struvite nucleation. It was found that induction time decreased with an increase in supersaturation, temperature and pH but increased with the presence of excess chloride (Cl^-) ion. Interfacial energy of two nucleation mechanisms ($\gamma_{s,hom}$ and $\gamma_{s,het}$), homogeneous and heterogeneous, increased with an increase in solution pH for all temperatures whereas interfacial energy of crystals increased with decrease in temperature. Thermodynamic parameters such as activation energy and interfacial energy were calculated based on rate of nucleation for both homogeneous and heterogeneous crystallisation. Finally, inhabitation of struvite nucleation by presence of foreign ion has been reported here.

Keywords: Saturation index; Induction time; Homogeneous nucleation; Heterogeneous nucleation; Struvite; Wastewater treatment plan

1. Introduction

Struvite is chemically known as magnesium ammonium phosphate hexahydrate ($MgNH_4PO_4.6H_2O$). Struvite usually precipitates as stable white crystals in a 1:1:1 M ratio according to the following reaction [1] where n can be 0, 1 or 2:

$$Mg^{2+} + NH_4^+ + H_nPO_4^{n-3} + 6H_2O \rightleftarrows MgNH_4PO_46H_2O + nH^+ \quad (1)$$

Magnesium, ammonium and phosphate ions are released as the result of solids degradation in an anaerobic digestion of wastewater treatment plant. Under certain physico-chemical conditions, these dissolved wastewater constituents can combine to form struvite according to Eq. (1) which causes scale deposition on pipe walls, pump and equipment surfaces of anaerobic digestion and post-digestion processes. The blockage of pipes leads to an increase in pumping cost and also reducing plant capacity [2]. It is not only pipes that are affected by struvite deposits, centrifuges, pumps, heat exchanger and aerators are

---

*Corresponding author.

1944-3994/1944-3986 © 2013 Balaban Desalination Publications. All rights reserved.

also prone to fouling by struvite. Primarily, as a problem to eliminate or inhibit struvite formation [2], struvite also offers itself as a fertilizer which encourages wastewater treatment companies to study its possible recovery [3]. For those two reasons, it has become important to study the principles of struvite nucleation and to assess the various controlling physico-chemical parameters on struvite crystallisation. Predicting struvite precipitation potential is critical to designer and operators for anticipating potential struvite formation problems and for remediating existing struvite damage. Struvite precipitation can be separated into two basic stages: nucleation and growth. Nucleation occurs when ions combine to form crystal embryos that can act as the foundation for growth into detectable crystals [4]. Crystal growth continues until equilibrium is reached [2]. Predicting and controlling of these two stages is complex as it is controlled by a combination of factors including thermodynamics of liquid–solid equilibrium, phenomena of mass transfer between solid and liquid phases and kinetics of reaction. There are also various physico-chemical parameters such as solution pH, supersaturation, temperature, interfacial energy, agitation energy and presence of other interfering ions [1,5–8] strongly influence the mechanism of nucleation of struvite crystal. Increases in temperature or supersaturation, or a decrease in the interfacial energy are expected to produce an increased nucleation rate [9,10]. Homogeneous nucleation occurs spontaneously, whereas heterogeneous nucleation takes place due to presence of impurity particles and secondary nucleation occurs in the presence of seed crystals. The time taken for nucleation to occur where duration from the achievement of supersaturation to the appearance of crystal nuclei (often termed the induction time) has been reported to dictate the formation of a precipitate and hence scaling formation [2]. Söhnel and Garside [11] presented the development of a fundamental model to describe crystal nucleation and growth during the induction period, which, they reported, accurately predicts the observed behaviour of many moderately and sparingly soluble crystal precipitates. Various indicators have been used for the determination of crystallization induction period: observation of light scintillations [4,12], conductivity measurement [13], pH monitoring [7,14] and absorbance measurements [13]. Each and every method has their own advantages and limitations. However, little is known about its tendency to nucleate and precipitate. Bouropoulos and Koutsoukos [15] and Ohlinger et al. [16] reported that struvite nucleation is inversely proportional to the supersaturation ratio (Ω). The pH, agitation energy, supersaturation and the presence of foreign ions are the important factors affecting induction time [7]. The reduction of induction time with an increase in solution pH and temperature was also reported by Bhuiyan et al. [7]. Temperature has a direct influence on the solubility of struvite and thermodynamics properties [17] and hence nucleation rate. The pH range within which struvite can precipitate was identified as 7–11 [18]. The influence of pH and supersaturation on the precipitation rate and crystal characteristics of struvite has been demonstrated by several investigators [1,2,7] but as yet little interest has been given to the influence of foreign ions on struvite nucleation and crystallization. Theoretically, impurities in solution can affect the nucleation and growth rate of crystals due to blocking of active growth sites inhibiting the increase of crystal size [1]. In the case of struvite crystallisation from wastewater sludge, foreign compounds such as potassium, chloride, calcium carbonate and zinc are numerous. There are few reported results on the effects of impurities such as chloride ion [1,15], carbonate ions [1], fluoride ion [19] and ethylenediaminetetraacetic acid [20] on struvite precipitation from synthetic supersaturated solution. Impurity molecules adsorb onto the nucleus surface can result in change of interfacial energy and nucleation rate. To further examine nucleation behaviour, this study was undertaken to estimate nucleation rate parameters of struvite formation in a stirred batch crystalliser while examining the influence of pH, temperature, supersaturation and salt (NaCl and KCl) impurities on nucleation. The activation and interfacial energies during struvite formation may be determined from the experimental results which will give a better understanding of the phenomenon.

1.1. Theory on calculation of the saturation index

Supersaturations index (SI) of solution values were calculated by the PhreeqC model. The supersaturation ratio Ω is given by:

$$\Omega = \frac{{}^{a}\mathrm{Mg}^{2+} \cdot {}^{a}\mathrm{NH}_4^{+} \cdot {}^{a}\mathrm{PO}_4^{3-}}{K_{\mathrm{sp}}} \tag{2}$$

According to Bhuiyan et al. [21], the thermodynamic solubility product of struvite on equilibrium with pure and solid phase struvite is as follows:

$$K_{\mathrm{sp}} = \{\mathrm{Mg}^{2+}\}\{\mathrm{NH}_4^{+}\}\{\mathrm{PO}_4^{3-}\} \tag{3}$$

$$K_{sp} = \gamma_{Mg^{2+}}[Mg^{2+}]\cdot\gamma_{NH_4^+}[NH_4^+]\cdot\gamma_{PO_4^{3-}}[PO_4^{3-}] \quad (4)$$

$$K_c = [Mg^{2+}][NH_4^+][PO_4^{3-}] \quad (5)$$

where $\{Mg^{2+}\}$, $\{NH_4^+\}$ and $\{PO_4^{3-}\}$are the ion activity of magnesium, ammonium and phosphate, respectively; $[Mg^{2+}]$, $[NH_4^+]$ and $[PO_4^{3-}]$ are the concentration of the ion magnesium, ammonium and phosphate, respectively; and $\gamma_{Mg^{2+}}$, $\gamma_{NH_4^+}$ and $\gamma_{PO_4^{3-}}$ are the activity coefficient of the ion magnesium, ammonium and phosphate, respectively; K_{sp} is the solubility product in terms of ion activity; and K_c is the solubility product in terms of concentration.

The SI value for sturvite is used as an indication of supersaturation. If the SI is negative, the system is undersaturated with respect to struvite. If the SI is positive, the solution is supersaturated. The SI values were calculated for all the experiments using the PhreeqC model. PhreeqC is a computer program designed based on an ion-association aqueous model for simulating chemical reaction in polluted water [22]. Moreover, PhreeqC provides well-established thermodynamic databases which can be used depending on user specification [23].

$$SI = \log\Omega = \log\frac{\frac{[Mg^{2+}][NH_4^+][PO_4^{3-}]}{K_{sp}}}{\gamma_{Mg^{2+}}\cdot\gamma_{NH_4^+}\cdot\gamma_{PO_4^{3-}}} \quad (6)$$

$$\log K_{sp} = -1157.45 - 0.784T - \frac{63.86}{T} + 556.83\log T + \frac{19.54}{T^2} \quad (7)$$

The equilibrium and the corresponding stability constants used for supersaturation calculation are summarised from Martell et al. [24] and Bhuiyan et al. [23].

2. Materials and methods

2.1. Synthetic liquor preparation

In this study, synthetic supernatant containing the constituent ions of struvite was used. The reagent salts used to prepare the synthetic liquor were analytical grade magnesium chloride ($MgCl_2$) and ammonium dihydrogen phosphate ($NH_4H_2PO_4$). Sodium chloride (NaCl) was used as additive and sodium hydroxide (NaOH) was used to adjust solution pH. $MgCl_2$ was obtained from Sigma and $NH_4H_2PO_4$ was obtained from Perth Scientific Australia. All chemicals were of analytical grade and were used without further treatment. Double-distilled water was used for all solution preparation. pH was measured by an Orion pH meter.

2.2. Batch experimental procedure

The experimental apparatus used in the study is shown in Fig. 1. An Erlenmeyer flask of 250 ml was placed in the water bath containing water. A stainless steel holder was used to keep the flask in place and a magnetic stirrer was used to stir the solution inside the flask. The water bath was maintained at a constant temperature by recirculating water through a pump which formed part of the cryothermostat. Water is maintained at a given temperature in the cryothermostat.

In each experiment, the supersaturated solution was prepared by mixing equimolar quantities of Mg^{2+}, NH_4^+ and PO_4^{3-}. The desired quantity of $NH_4H_2PO_4$ solution were poured into an Erlenmeyer flask (working volume = 100 ml), and mixed by a magnetic stirrer. To avoid evaporation, the Erlenmeyer flask was closed by using a rubber stopper, and sealed with paraffin film. After the solution has achieved the desired temperature (within ± 0.01 C), a required quantity of $MgCl_2$ solution at the same temperature was added into the Erlenmeyer flask 0.1 M solution of NaOH was added by using a syringe to achieve the desired pH. The time that elapsed between pH adjustment, and the first pH observed change is defined as the induction time. The experiment was stopped after the pH attained a new constant value. The experiments were conducted at different initial pH of 8 and 8.5.

For studying additive effect, the same procedure was used except that a predetermined concentration of NaCl or KCl was added into the Erlenmeyer flask before the addition of $MgCl_2$. The solution condition was kept at pH 8. The concentration of NaCl in the

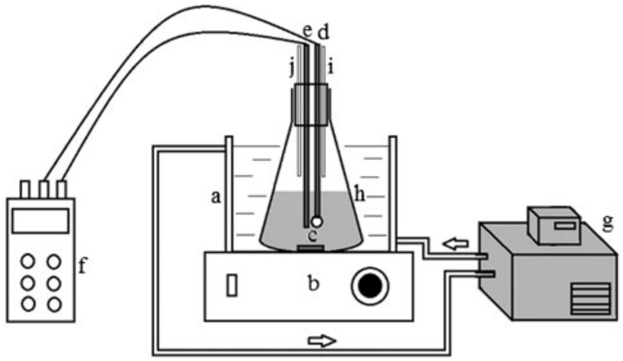

Fig. 1. The experimental set-up; (a) water bath, (b) magnetic stirrer, (c) magnetic rotor, (d) pH electrode, (e) thermometer, (f) pH meter, (g) cryothermostat, (h) Erlenmeyer flask, (i) for NaOH dosing and (j) for magnesium dosing.

Erlenmeyer flask varied between 8.06 and 16.38 mM after mixing of $MgCl_2$ and $NH_4H_2PO_4$; therefore, the concentration of Cl^- ranged from 12.54 to 25.48 mMol. The excess Cl^- ions can be defined as follows:

$$E = \frac{[Cl^-] - [Cl^-_{eqm}]}{[Cl^-_{eqm}]} \tag{8}$$

where Cl^- is the molar concentration of chloride in solution and Cl^-_{eqm} is the chloride introduced in solution through the equimolar feed as $MgCl_2$. The additive effect studies was carried out for a fixed value of excess chloride added as NaCl or KCl, namely $E = 0.4$.

The range of supersaturation was varied from 1.02 to 1.45 for all experiments. Three temperature levels (20, 25 and 30℃) were used for struvite nucleation study. The PhreeqC model was used for calculating the supersaturation of struvite varying from 0.00–16.38 mMol Cl^- ions solution at 20–30℃. The calculated results are tabulated in Tables 1 and 2.

3. Results and discussions

3.1. Effect of pH on spontaneous nucleation of struvite crystals

pH is one of the important driving forces controlling the formation of struvite [2,25]. The initial experiments undertaken used pH as an indicator of struvite nucleation. As the struvite precipitates, it triggers a release of proton ions in solution, and hence, a change in pH occurs during the nucleation process. The drop in pH is characteristic of the onset

Table 1
The supersaturation of struvite without the addition of NaCl, $E = 0$

pH 8			pH 8.5		
$MgCl_2$ (mM)	$NH_4H_2PO_4$ (mM)	SI	$MgCl_2$	$NH_4H_2PO_4$ (mM)	SI
$T = 20$℃					
4.35	4.35	1.02	2.65	2.65	1.02
4.55	4.55	1.06	2.75	2.75	1.06
4.65	4.65	1.09	2.83	2.83	1.09
4.85	4.85	1.13	2.93	2.93	1.13
5.10	5.10	1.18	3.10	3.10	1.18
5.50	5.50	1.25	3.32	3.32	1.25
5.95	5.95	1.33	3.60	3.60	1.33
6.35	6.35	1.39	3.82	3.82	1.39
6.75	6.75	1.45	4.06	4.06	1.45
$T = 25$℃					
5.10	5.10	1.02	3.10	3.10	1.02
5.30	5.30	1.06	3.23	3.23	1.06
5.50	5.50	1.09	3.32	3.32	1.09
5.70	5.70	1.13	3.45	3.45	1.13
6.00	6.00	1.18	3.63	3.63	1.18
6.50	6.50	1.25	3.90	3.90	1.25
7.00	7.00	1.33	4.24	4.24	1.33
7.50	7.50	1.39	4.50	4.50	1.39
8.00	8.00	1.45	4.80	4.80	1.45
$T = 30$℃					
5.60	5.60	1.02	3.42	3.42	1.02
5.85	5.85	1.06	3.56	3.56	1.06
6.00	6.00	1.09	3.68	3.68	1.09
6.30	6.30	1.13	3.84	3.84	1.13
6.60	6.60	1.18	4.05	4.05	1.18
7.15	7.15	1.25	4.35	4.35	1.25
7.75	7.75	1.33	4.70	4.70	1.33
8.30	8.30	1.39	5.00	5.00	1.39
8.80	8.80	1.45	5.30	5.30	1.45

Table 2
The supersaturation of struvite with the addition of NaCl and KCl at pH 8, $E = 0.4$

$MgCl_2$ (mM)	$NH_4H_2PO_4$ (mM)	NaCl or KC (mM)	SI
$T = 20$°C			
4.48	4.48	8.06	1.02
4.65	4.65	8.37	1.06
4.80	4.80	8.64	1.09
5.00	5.00	9.00	1.13
5.30	5.30	9.54	1.18
5.68	5.68	10.22	1.25
6.20	6.20	11.16	1.33
6.55	6.55	11.79	1.39
7.00	7.00	12.60	1.45
$T = 25$°C			
5.25	5.25	9.45	1.02
5.50	5.50	9.90	1.06
5.65	5.65	10.17	1.09
5.90	5.90	10.62	1.13
6.20	6.20	11.16	1.18
6.70	6.70	12.06	1.25
7.25	7.25	13.05	1.33
7.75	7.75	13.95	1.39
8.25	8.25	14.85	1.45
$T = 30$°C			
5.80	5.80	10.44	1.02
6.00	6.00	10.80	1.06
6.20	6.20	11.16	1.09
6.50	6.50	11.70	1.13
6.85	6.85	12.33	1.18
7.35	7.35	13.23	1.25
8.00	8.00	14.40	1.33
8.55	8.55	15.39	1.39
9.10	9.10	16.38	1.45

of nucleation at which the first crystals of struvite occurs and is linked to the rate of struvite nucleation.

The effect of the initial solution pH on induction time was investigated at the same initial supersaturation with a molar ratio of Mg, NH_4 and PO_4 ion concentration in solution of 1:1:1. Fig. 2 shows the variation of induction time with solution pH for various selected initial supersaturations. It was found that induction time decreased with increase in solution pH (Fig. 2). This reduction of induction time was more pronounced at pH of 8.5 compared to a pH of 8 (Fig. 2).

Fig. 2 also shows the effect of excess Cl^- in the form of NaCl addition. For any given solution pH, the presence of NaCl resulted in higher induction time (Fig. 2). The presence of Cl^- ions may affect equilibrium solubility, solution structure and complex formation [9] and hence interference on nucleation. Similar observation was reported by Söhnel and Mullin [26] for $CaCO_3$ crystal formation and it was found that an increase in the crystal–solution interfacial energy is due to the presence of foreign ions.

3.2. *Effect of supersaturation on spontaneous nucleation of struvite crystals*

To study the effect of supersaturation, experiments were conducted with changes of supersaturation index (SI = 1.02 to 1.33) at a constant temperature of 25°C. Fig. 2 also shows the effect of supersaturation and initial solution pH on induction time. It was found that induction time decreased with increase in supersaturation at any particular initial solution pH. The rapid rate of nucleation for higher supersaturation is due to a higher driving force for mass transfer from liquid to crystal phase.

3.3. *Effect of temperature on kinetics of struvite nucleation*

The induction time is strongly affected by both the temperature and supersaturation of the solution. Batch experiments were investigated for temperatures of 20, 25 and 30°C. Table 3 represents the variation of induction times obtained at various levels of initial supersaturation and temperatures at pH 8. It was found that increase in supersaturation substantially decreases the induction period for all temperatures. For a given supersaturation, the induction time decreased with increase in temperature. According to the classical nucleation theory, the decrease in induction time at higher solution temperature is caused not only by the effect of temperature but also by the smaller interfacial energy of crystals [9,27].

For the effect of temperature on any rate processes, such as nucleation, an Arrhenius equation is commonly used. The activation energy of nucleation, E_{act}, can be calculated by the following Arrhenius equation:

$$\frac{d \ln k_N}{dT} = \frac{-E_{act}}{RT^2} \tag{9}$$

By the integration of Eq. (9):

$$k_N = k_0 \cdot \exp\left(\frac{-E_{act}}{RT}\right) \tag{10}$$

This empirical equation has been simplified by Cheng and Li [28], so:

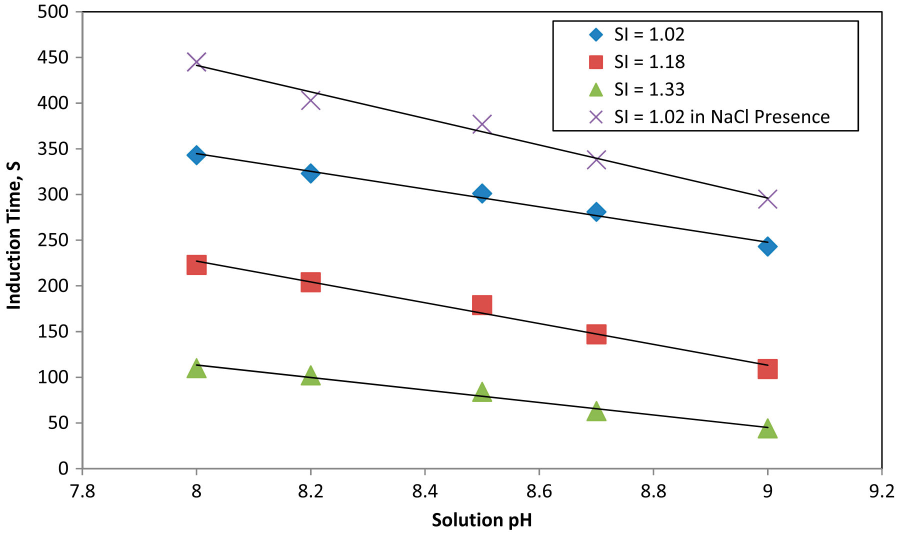

Fig. 2. Variation of induction time with initial pH and SI at 25°C.

Table 3
Induction time on spontaneous nucleation of struvite crystals with various temperature and SI at pH 8

Temperature	Induction time, s		
	SI = 1.02	SI = 1.18	SI = 1.33
20	432	261	139
25	343	223	110
30	271	173	96

$$t_{\mathrm{ind}} = \tau.\exp\left(\frac{-E_{\mathrm{act}}}{RT}\right) \tag{11}$$

$$\log\frac{1}{t_{\mathrm{ind}}} = \log\tau\frac{-E_{\mathrm{act}}}{2.303\,RT} \tag{12}$$

where τ is a constant, E_{act} is the activation energy ($\mathrm{J\,mol^{-1}}$) for the process, and R is the gas constant (8.314 J/K mol). Activation energy represents the minimum energy that is required for a chemical reaction to take place. Fig. 3(a) and (b) is a plot of log ($1/t_{\mathrm{ind}}$) vs. 1,000/T for three different initial levels of supersaturation. From the slope of these straight lines, the average values of E_{act} of 30.1 and 24.9 $\mathrm{kJ.mol^{-1}}$ were obtained at pH 8 and 8.5, respectively. Similar range of values of activation energy for nesquehonite ($MgCO_3{\cdot}3H_2O$) and ammoniumsilicate was also reported by Cheng and Li [28] and Zang et al. [29], respectively.

An equation developed by Nielsen [30], Nývlt [31] and Söhnel and Garside [11] for calculation of homogeneous nucleation rate is as follows:

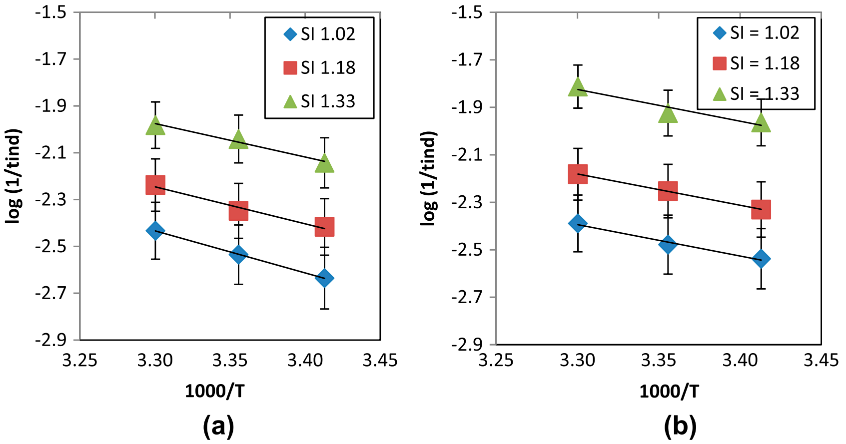

Fig. 3. Dependence of induction time on temperature; (a) pH = 8 and (b) pH = 8.5.

$$J = k_N \Omega^n \quad (13)$$

where k_N is the nucleation rate constant and n is the kinetic order of nucleation.

A simplifying assumption was used that the induction time may be considered to be inversely proportional to the rate of nucleation. So induction period (t_{ind}) may be used to determine the nucleation rate (J) [8].

$$J = \frac{k}{t_{ind}} \quad (14)$$

where K is a constant. Combining Eqs. (13) and (14) results in Eq. (15):

$$t_{ind} = \left(\frac{k}{k_N}\right) \cdot \Omega^{-n} \quad (15)$$

$$\frac{k}{k_N} = K \quad (16)$$

The semi empirical correlation of induction time on supersaturation Eq. (15) can be simplified into Eq. (17) below and the data plotted in Fig. 4.

$$\log t_{ind} = \log K - n \log \Omega \quad (17)$$

where K and n are empirical constants obtained via straight line fitting to experimental data in Fig. 4.

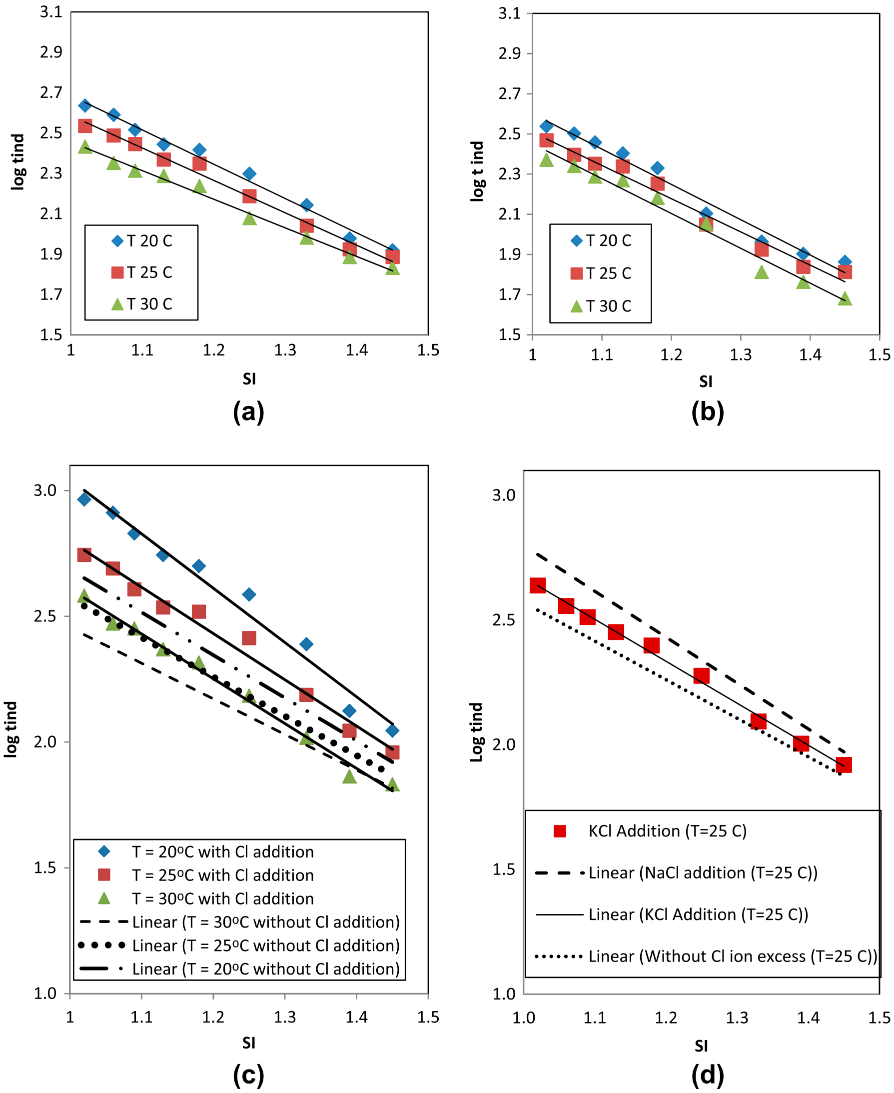

Fig. 4. Induction time as a function of initial supersaturation and at different temperatures; (a) pH 8, (b) pH 8.5, (c) pH 8 with NaCl addition and (d) pH 8 with and without NaCl and KCl addition.

Table 4
Various kinetic parameters on struvite nucleation

Calculated from Eq. (15)				Calculated from Eqs. (17) and (19)			
T (℃)	K	n	R^2	B_{het}	B_{hom}	γ_{het} (mJ m^{-2})	γ_{hom} (mJ m^{-2})
pH 8.0 without Cl^- ion addition							
20	24,320	1.7	0.96	0.98	2.14	15.67	20.37
25	15,600	1.6	0.98	0.83	1.97	15.08	20.13
30	7,450	1.4	0.97	0.77	1.66	14.97	19.33
pH 8.5 without Cl^- ion addition							
20	22,800	1.7	0.96	0.86	1.92	15.05	19.62
25	14,500	1.6	0.97	0.82	1.83	15.04	19.65
30	17,420	1.83	0.97	0.76	1.71	14.89	19.54
pH 8 with NaCl addition							
20	189,850	2.2	0.98	1.26	2.86	18.74	22.42
25	43,740	1.8	0.97	1.01	2.43	16.14	21.60
30	20,240	1.7	0.97	1.07	2.11	16.71	20.95
pH 8 with KCl addition							
20	61,720	1.9	0.98	1.12	2.38	16.41	21.09
25	21,880	1.7	0.97	0.98	2.02	15.96	20.31
30	16,200	1.6	0.98	0.90	1.90	15.77	20.23

The dependence of the induction time on supersaturation is shown in Fig. 4(a) and (b) for pH 8 and 8.5, respectively. The fitting parameters from Fig. 4(a) and (b) are presented in Table 4. Nucleation was higher at high temperature for all solution pH ranges resulted by lower induction time and lower interfacial energy (Table 4).

3.4. Inhabitation of spontaneous nucleation of struvite due to presence of excess chloride ions

In this study, the excess Cl^- ions were obtained in a batch experiment at pH 8 by adding sodium chloride (NaCl) or potassium chloride (KCl). The experimental data of induction time obtained at different supersaturations with and without the addition of excess Cl^- ions at pH 8 are shown in the log t_{ind} – SI plots of Fig. 4(a)–(d) for $E = 0$ and 0.4, respectively. The results showed that the induction time continuously decreased with increasing supersaturation. The effect of excess CI^- ions in a solution showed that induction time increased in the presence excess Cl^- ions. Fig. 4(d) shows that the effect of excess Cl^- ions on the induction time is more significant at lower supersaturations. In general, the effect of excess Cl^- ions in a solution may affect the induction time considerably [9]. This may be due to adsorption or chemisorption of foreign ions on nuclei or heteronuclei, by changing the equilibrium solubility or by the solution structure, by chemical reaction or by complex formation in the solution [9].

The various calculated nucleation kinetic parameters (K and n) are tabulated in Table 4. It can be seen that the empirical constants, K, are larger at lower temperatures. When compared with the data at pH 8 without presence of excess Cl^- in Table 4, the effect of excess Cl^- can significantly increase empirical constant K values and nucleation order n.

For comparison purpose, two forms of excess Cl^- ions, in the form of either NaCl or KCl were used. Fig. 4(d) shows the effect of KCl and NaCl on the induction time. It can be seen that, for fixed value of supersaturation, the presence of excess chloride ions in solution has a strong retarding effect on induction time, Na^+ ions having a more significant inhibition than K^+. This is because of different ionic radius and ionic charges. Fig. 5 gives the effect of Na^+ and K^+ on the induction time for $SI = 1.02$. It can be seen that the presence of Na^+ and K^+ ions in solution affects the behaviour of the induction time, increasing with NaCl and KCl concentration up to a maximum at about E of 0.1–0.3, and reduces thereafter at higher E values. A comparison between Na^+ and K^+ ion for the same range of excess Cl^- ions shows that the influence of Na^+ in increasing the induction time is stronger than that of K^+ over all concentration ranges.

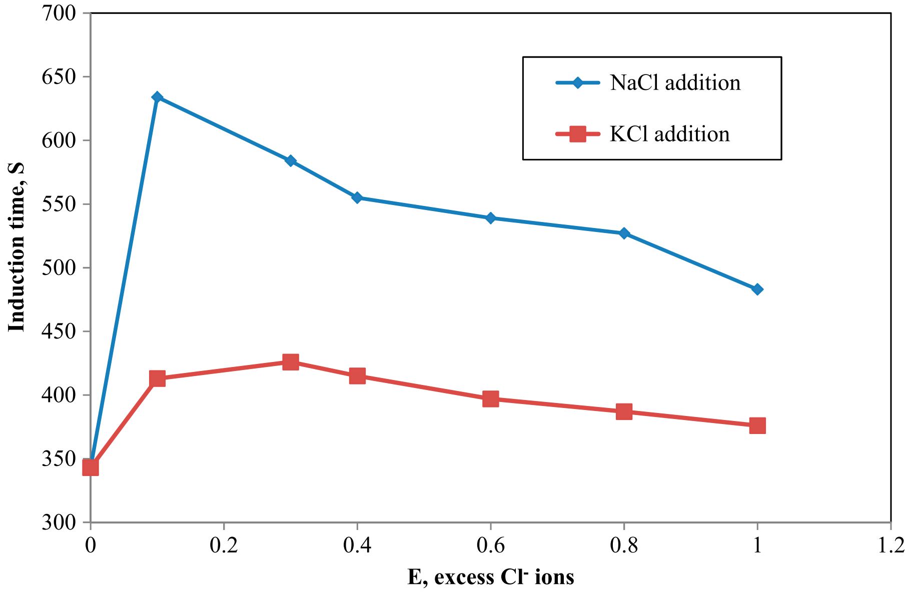

Fig. 5. Effect of Na^+ and K^+ on the induction time on SI = 1.02 at 25˚C and pH 8.

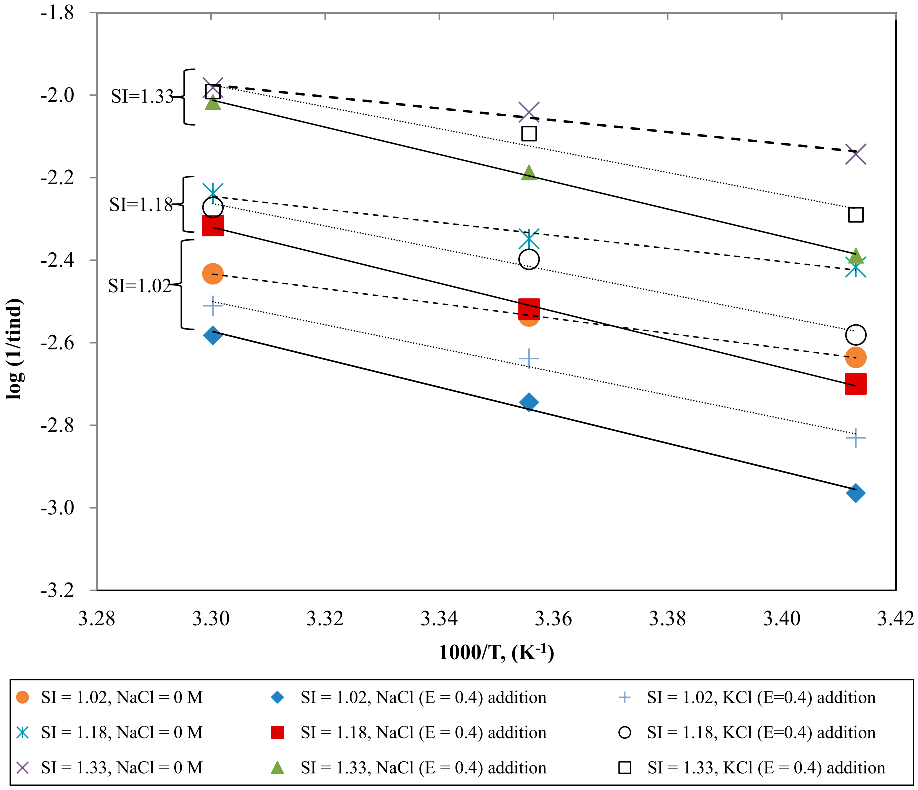

Fig. 6. Dependence of the induction time on the inverse of temperature at pH 8 and with and without the presence of NaCl.

The plotting of Eq. (12) for three different levels of supersaturation is shown in Fig. 6 for the effect of the presence of excess chloride. The same linear relationship was compared with those shown in Fig. 4 (a), and reproduced in Fig. 6. The slope of the straight line is higher when excess chloride is present, suggesting that with excess chloride ions in either NaCl or KCl, there is more inhibition for nucleation than in the case of equimolarity [32] where no NaCl or KCl was added. From the slope of these straight lines, the average activation energies are 64.5 and 51.7 kJ mol^{-1} for NaCl and KCl addition, respectively. These values are much higher than the case with no NaCl and KCl added (30.1 kJ mol^{-1}). This shows that foreign ions increase the activation energy for struvite nucleation, showing that primary nucleation of struvite can be inhibited by the presence of excess chloride ions such as NaCl and KCl. The activation energy in the presence of NaCl was higher than in the presence of KCl.

3.5. Mechanism of nucleation and thermodynamic parameters

The nucleation rate J (cm^{-3} s^{-1}) based on classical homogeneous nucleation theory can be expressed as follows:

$$J = A \exp\left[-\frac{\beta \cdot \gamma_S^3 \cdot V_m^2 \cdot N_A}{(RT)^3 \cdot (\ln S)^2}\right] \tag{18}$$

where A is the frequency constant, β is the geometric factor (for cube is 32), N_A is the Avogadro number, R is the gas constant, V_m is the molar volume, S is activity-based supersaturation ratio, T is the absolute temperature and γ_s the interfacial energy.

The induction time can be related to the supersaturation by:

$$\log t_{ind} = A + \frac{B}{(\log \Omega)^2} \tag{19}$$

where A and B are constants according to the classical theory:

$$B = \frac{\beta \cdot \gamma_S^3 \cdot V_m^2 \cdot N_A}{(2.303RT)^3} \tag{20}$$

where υ_m is the molecular volume of struvite (=molar volume/(Avogadro's number x density x number of ions in formula unit) = 7.99 × 10^{-23}cm^3/mol) and β is a geometric factor (=32 for cubes), so:

$$B = \frac{\beta \cdot \gamma_S^3 \cdot V_m^2}{(2.303RT)^3} \tag{21}$$

The interfacial tension γ_S is:

$$\gamma_s = 2.3RT\left(\frac{B}{\beta \cdot \upsilon_m^2}\right)^{1/3} \tag{22}$$

The validity of Eq. (19) is based on the assumption that nucleation time is much greater than the growth time ($t_n >> t_g$) [33]. Then the induction period can be used to represent the time needed for critical nuclei formation. To verify whether this was the case for struvite, log t_{ind} was plotted vs. SI as shown in Fig. 7. It can be seen that the measured induction time for struvite crystallization followed a linear relationship given by Eq. (17). Fig. 7 illustrates two characteristics of nucleation. Region II for low supersaturation is characteristic of heterogeneous nucleation mechanism; Region I for high supersaturations indicates homogeneous nucleation mechanism dominates.

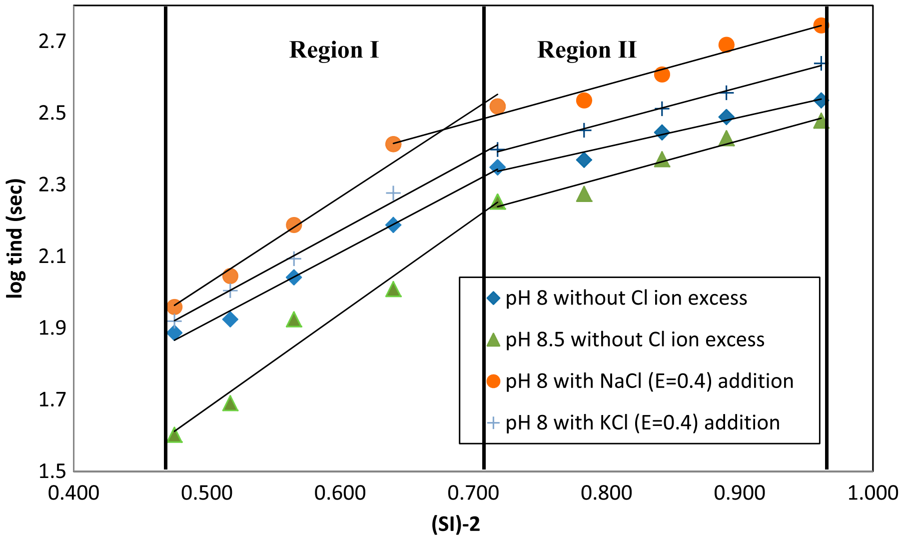

Fig. 7. Induction period as a function of supersaturation at 20°C with and without excess Cl^{-} ions.

The data resulted in two distinct linear parts showing the dependence of nucleation on different nucleation mechanisms. Homogeneous nucleation region has higher slope and occurred at higher supersaturations and the region of lower slope occurred at lower supersaturations due to heterogeneous nucleation [11]. The value of the slope of B_{hom} is higher than B_{het} as given in Table 4. The nucleation is largely homogeneous at high supersaturation, while heterogeneous nucleation prevails at supersaturation up to 1.18 for all temperature and pH ranges studied. This transition from homogeneous to heterogeneous nucleation is not affected by the presence of excess chloride ions. In this paper, Fig. 7 only showed one temperature at 20°C. Similar plots were made for temperatures of 25 and 30°C (not shown here) and their calculated corresponding values are listed in Table 4.

The value of B_{hom} is consistently higher than B_{het} for all experimental data. Calculated results of interfacial energy for two nucleation mechanisms ($\gamma_{\mathrm{s,hom}}$ and $\gamma_{\mathrm{s,het}}$) in Table 4 indicate that interfacial energies decrease with higher solution pH and for higher temperatures. For any given solution pH, interfacial energy of crystals increases with decrease in temperature. This is consistent that interfacial energy impacts on induction time. The effect of excess chloride shows that interfacial energy increases with its presence at all temperatures. The inhibition effect of added NaCl and KCl may be due to complex ion formation or due to foreign ion adsorbed onto nuclei surface.

A comparison of the interfacial energy derived from this study compares very well with results of Bouropoulos and Koutsoukos [15] but much larger than others [4,7,14]

3.6. Crystal Morphology at different solution pH with and without NaCl and KCl addition

The micropictures of crystals, shown in Fig. 8, obtained in the experiments were investigated by using an optical microscope. The crystal morphologies form pH 8 and 8.5 showed similar crystal shapes and dimensions (see Fig. 8(a) and 8(b), respectively). The shape of crystals on pH 8 and 8.5 exhibited needle-like crystals. The crystals in the presence of NaCl and KCl, shown in Fig. 8(c) and 8(d), respectively, were similar in shape with those shown in Fig. 8(a). The morphology in all the different cases, different pH and the presence or absence of excess Cl^- ions remain the same, being needle-like in structure.

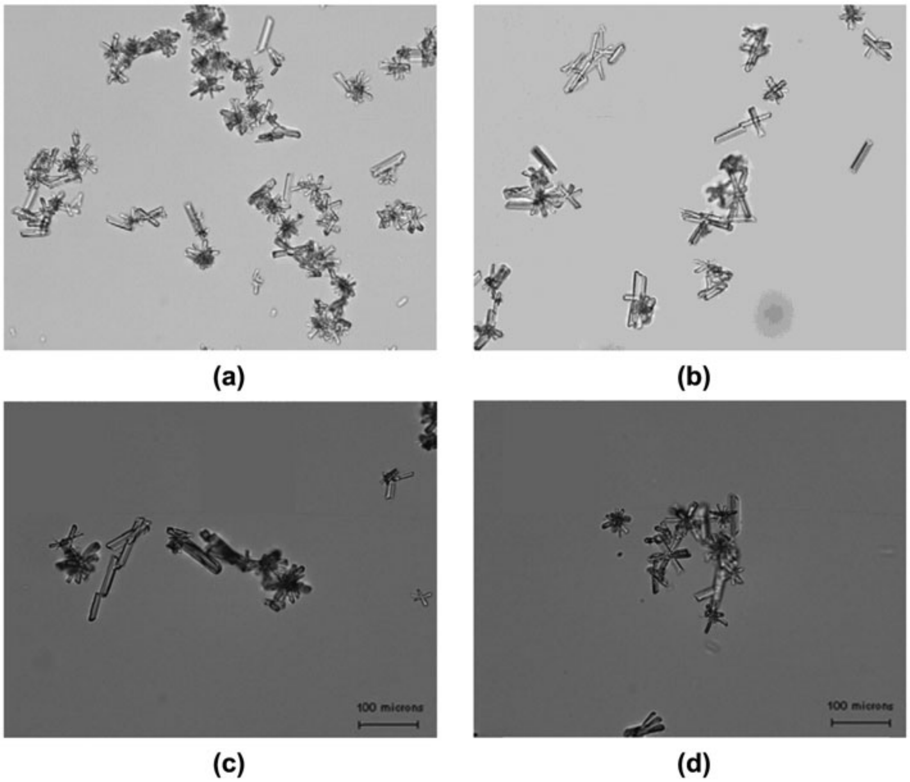

Fig. 8. Morphology of struvite crystals obtained in experiments based on the same magnification: (a) pH 8, (b) pH 8.5, (c) pH 8 with NaCl addition and (d) pH 8 with KCl addition.

4. Conclusions

The impact of various physico-chemical parameters, such as solution pH, supersaturation, temperature and the presence of foreign ion, on nucleation of struvite crystals are reported here.

The results indicated that the induction time decreased with an increasing pH, temperature and degree of supersaturation. The presence of excess chloride in the form of NaCl and KCl has an inhibitory effect on the nucleation of struvite.

The classical nucleation theory is applicable to explain the effect of various physico-chemical parameters on struvite nucleation. The activation energy for struvite nucleation was calculated as 30.1 and 24.9 kJ.mol^{-1} at pH 8 and 8.5, respectively. The lower activation energy at pH 8.5 accounts for the shorter induction time obtained at pH 8.5. The activation energies in the presence of NaCl and KCl were higher (64.5 and 51.7 kJ/mol, respectively) at pH 8. The higher activation energy with NaCl and KCl addition can account for their inhibitory effect. The interfacial energy between struvite crystals and supersaturated solution decreased with increase in pH but increased in the presence of either NaCl or KCl. The morphology at different pH and the presence or absence of excess Cl$^-$ ions are similar, being needle-like in structure.

References

[1] K.S.L. Corre, E. Valsami-Jones, P. Hobbs, S.A. Parsons, Impact of calcium on struvite crystal size, shape and purity, J. Cryst. Growth 283 (2005) 514–522.

[2] J.D. Doyle, S.A. Parsons, Struvite formation, control and recovery, Water Res. 36 (2002) 3925–3940.

[3] K.S.L. Corre, E. Valsami-Jones, P. Hobbs, B. Jefferson, S.A. Parsons, Agglomeration of struvite crystals, Water Res. 41 (2007) 419–425.

[4] K.N. Ohlinger, T.M. Young, E.D. Schroeder, Kinetics effects on preferential struvite accumulation in wastewater, J. Environ. Eng. 125 (1999) 730–737.

[5] S. Uludag-Demirer, G.N. Demirer, S. Chen, Ammonia removal from anaerobically digested dairy manure by struvite precipitation, Process Biochem. 40 (2005) 3667–3674.

[6] K.N. Ohlinger, T.M. Young, E.D. Schroeder, Predicting struvite formation in digestion, Water Res. 32 (1998) 3607–3614.

[7] M.I.H. Bhuiyan, D.S. Mavinic, R.D. Beckie, Nucleation and growth kinetic of struvite in a fluidized bed reactor, J. Cryst. Growth 310 (2008) 1187–1194.

[8] W.C. Chien, C.Y. Tai, J.P. Hsu, The induction period of the CaCl2– Na2CO3 system: Theory and experiment, J. Chem. Phys. 111 (1999) 2657–2664.

[9] J.W. Mullin, Crystallization, 4th ed., Butterworth-Heinemann, Oxford, 2001.

[10] R.A. Judge, R.S. Jacobs, T. Frazier, E.H. Snell, M.L. Pusey, The effect of temperature and solution pH on the nucleation of tetragonal lysozyme crystals, Biophys. J. 77 (1999) 1585–1593.

[11] O. Söhnel, J. Garside, Precipitation: Basic principles and industrial applications, Butterworth-Heinemann, Oxford, 1992.

[12] S.C. Galbraith, P.A. Schneider, A review of struvite nucleation studies, in: International Conference on Nutrient Recovery from Wastewater Streams, Vancouver, BC, Canada, 2009.

[13] I. Kabdasli, S.A. Parsons, O. Tünay, Effect of major ions on induction time of struvite precipitation, Croat. Chem. Acta 79 (2006) 234–251.

[14] A.N. Kofina, P.G. Koutsouko, Spontaneous precipitation of struvite from synthetic wastewater solutions, Cryst. Growth Des. 5 (2005) 489–496.

[15] N.C. Bouropoulos, P.G. Koutsoukos, Spontaneous precipitation of struvite from aqueous solutions, J. Cryst. Growth 213 (2000) 381–388.

[16] K.N. Olinger, T.M. Young, E.D. Schroedar, Kinetics effects on preferential struvite accumulation in wastewater, J. Environ. Eng. 125 (1999) 730–737.

[17] M. Ronteltap, M. Maurer, R. Hausherr, W. Gujer, Struvite precipitation from urine—Influencing factors on particle size, Water Res. 44 (2010) 2038–2046.

[18] A. Matynia, J. Koralewska, B. Wierzbowska, K. Piotrowski, The influence of process parameters on struvite continuous crystallization kinetics, Chem. Eng. Commun. 193 (2006) 160–176.

[19] H.D. Ryu, D. Kim, S.I. Lee, Application of struvite precipitation in treating ammonium nitrogen from semiconductor wastewater, J. Hazard. Mater. 156 (2008) 163–169.

[20] J.D. Doyle, K. Oldring, J. Churchley, C. Price, S.A. Parsons, Chemical control of struvite precipitation, J. Environ. Eng. 129 (2003) 419–426.

[21] Warmadewanthi, J.C. Liu, Recovery of phosphate and ammonium as struvite from semiconductor wastewater, Sep. Purif. Technol. 64 (2009) 368–373.

[22] D.L. Parkhurst, C.A.J. Appelo, User's guide To phreeqc (Version 2) – A computer program For speciation, batch-reaction, one-dimensional transport, and inverse geochemical calculations, Denver, Colorado, 1999.

[23] M.I.H. Bhuiyan, D.S. Mavinic, R.D. Beckie, A solubility and thermodynamic study of struvite, Environ. Technol. 28 (2007) 1015–1026.

[24] A. Martell, R. Smith, R. Motekaitis, NIST Critically selected stability constants of metal complexes, database version 5.0 NIST standard reference database 46 in, Texas A&M University, 1998.

[25] E. Ariyanto, H.M. Ang, T. Sen, Effect of initial solution pH on solubility and morphology of struvite crystals, in: Chemeca 2011, Sydney, New South Wales, Australia, 2011.

[26] O. Sohnel, J.W. Mullin, Precipitation of calcium carbonate, J. Cryst. Growth 60 (1982) 239–250.

[27] C.Y. Tai, W.C. Chien, Effects of operating variables on the induction period of CaCl2–Na2CO3 system, J. Cryst. Growth 237–239 (2002) 2142–2147.

[28] W. Cheng, Z. Li, Nucleation kinetics of nesquehonite ($MgCO_3{\cdot}3H_2O$) in the $MgCl_2-Na_2CO_3$ system, J. Cryst. Growth 312 (2010) 1563–1571.

[29] Y. Zhang, Y. Li, Y. Zhang, Supersolubility and induction of aluminosilicate nucleation from clear solution, J. Cryst. Growth 254 (2003) 156–163.

[30] A.E. Nielsen, Kinetics of Precipitation, Pergamon Press, New York, 1964.

[31] J. Nývlt, Industrial Crystallisation from Solutions, Butterworths, London, 1971.

[32] O.S. Pokrovsky, Precipitation of calcium and magnesium carbonates from homogeneous supersaturated solutions, J. Cryst. Growth 186 (1998) 233–239.

[33] O. Söhnel, J.W. Mullin, Interpretation of crystallization induction periods, J. Colloid Interface Sci. 123 (1988) 43–50.